

A major purpose of the Technical Information Center is to provide the broadest dissemination possible of information contained in DOE's Research and Development Reports to business, industry, the academic community, and federal, state and local governments.

Although a small portion of this report is not reproducible, it is being made available to expedite the availability of information on the research discussed herein.

1

CONF-840417--10

Los Alamos National Laboratory is operated by the University of California for the United States Department of Energy under contract W-7405-ENG-36.

LA-UR--84-3612

DE85 003775

TITLE: SOME THOUGHTS ON ALLOY DESIGN

MASTER

AUTHOR(S): P. L. Martin and J. C. Williams

REPRODUCTION OF THIS REPORT IS UNLIMITED WHEN REPRODUCED FOR PRIVATE COPY TO PERMIT THE DISSEMINATION OF INFORMATION OF THIS AVAILABILITY.

SUBMITTED TO: High Temperature Alloys: Theory and Design Symposium
April 1984

DISCLAIMER

This report was prepared as an account of work sponsored by an agency of the United States Government. Neither the United States Government nor any agency thereof, nor any of their employees, makes any warranty, express or implied, or assumes any legal liability or responsibility for the accuracy, completeness, or usefulness of any information, apparatus, product, or process disclosed, or represents that its use would not infringe privately owned rights. Reference herein to any specific commercial product, process, or service by trade name, trademark, manufacturer, or otherwise does not necessarily constitute or imply its endorsement, recommendation, or favoring by the United States Government or any agency thereof. The views and opinions of authors expressed herein do not necessarily state or reflect those of the United States Government or any agency thereof.

By acceptance of this article, the publisher recognizes that the U.S. Government retains a nonexclusive, royalty-free license to publish or reproduce the published form of this contribution, or to allow others to do so, for U.S. Government purposes.

The Los Alamos National Laboratory requests that the publisher identify this article as work performed under the auspices of the U.S. Department of Energy

REPRODUCTION OF THIS DOCUMENT IS UNLIMITED

Los Alamos Los Alamos National Laboratory
Los Alamos, New Mexico 87545

SOME THOUGHTS ON ALLOY DESIGN

P. L. Martin* and J. C. Williams**

*Los Alamos National Laboratory
Los Alamos, New Mexico 87545

**Carnegie-Mellon University
Pittsburgh, Pennsylvania 15213
USA

Summary

In this paper we discuss some of the problems associated with attempts to use first principles in alloy design. We briefly summarize the role of microstructure on the properties of high temperature alloys and illustrate some of the microstructural features of conventional superalloys. We also describe how theory and experiment are converging toward some predictive capabilities for relating microstructure and composition using Ni-Al-Mo-X alloys as an example. Finally, this paper suggests that progress is being made in combining the results of condensed matter theory and experimental research.

Introduction

The goals for the development of structural materials depend on the intended application of the alloy. In recent years it has become increasingly stylish to use the term "alloy design" in place of alloy development (1). An important issue becomes whether the use of this term is warranted and what it means to the different groups who use it. In some cases it means careful design of a statistically significant matrix of alloy compositions as the starting point for a detailed test program to determine the properties of all alloys in the matrix. In other cases it means using a knowledge of structure-property relations to select a particular microstructure which is known to exhibit attractive values of a particular property. Seldom does it mean the use of fundamental principles to formulate and process an alloy which has a particular microstructure and property set. Yet, this surely is what alloy design, in the strictest sense of the word, must mean. The reason that this is not generally possible is that the complexity of the intended application places a number of conflicting requirements on the performance of the alloy.

One possible exception is the high temperature class of alloys whose performance is limited by creep resistance more often than by any other property. In such cases, the task of designing an alloy becomes somewhat more tractable. There have been some notable examples of alloys which have been developed (but probably not designed) through an understanding of the mechanisms of creep and the principles of phase transformations/phase stability. In addition, processing to achieve a particular microstructure has been recognized in recent years; adding an additional tool for the use in microstructural synthesis.

The purpose of this paper is to describe the extent to which alloy design is presently possible. For both thematic reasons and for those described above, we will restrict our attention to high temperature alloys.

Background

Current high temperature Ni and Co-base alloys operate at temperatures in excess of $0.8 T_m$; such temperatures are much higher than other structural alloys can accommodate (2,3). This is possible for two principal reasons: the positive temperature dependence of the flow stress of the γ' precipitate and the ability to control grain boundary sliding either by modifying the microstructure at the boundary or by eliminating the boundaries altogether. This latter option is possible through creative processing schemes such as directional recrystallization, directional solidification, or single crystal growth.

There are basically three mechanisms that are responsible for the elevated temperature deformation of polycrystalline metals and alloys. These are dislocation glide, grain boundary sliding and diffusive flow. The overall deformation rate is the sum of these as expressed in equation 1.

$$\dot{\gamma}_t = \dot{\gamma}_{disL} + \dot{\gamma}_{gbs} + \dot{\gamma}_{diff} \quad (1)$$

In order to focus the attention on the rate controlling deformation modes, it has become popular to divide temperature-stress space into a number of regimes, each dominated by a single deformation mechanism. A plot of these regimes is known as a Deformation Mechanism Map (5,6), an example of which is shown in Figure 1. From this it can be seen that strengthening the grain interiors with respect to dislocation glide reduces the range of stress and temperature where this mechanism dominates and contracts the extent of the field labeled Plasticity. This substantially increases the strength of the alloy since the deformation rates in either the power law or diffusional

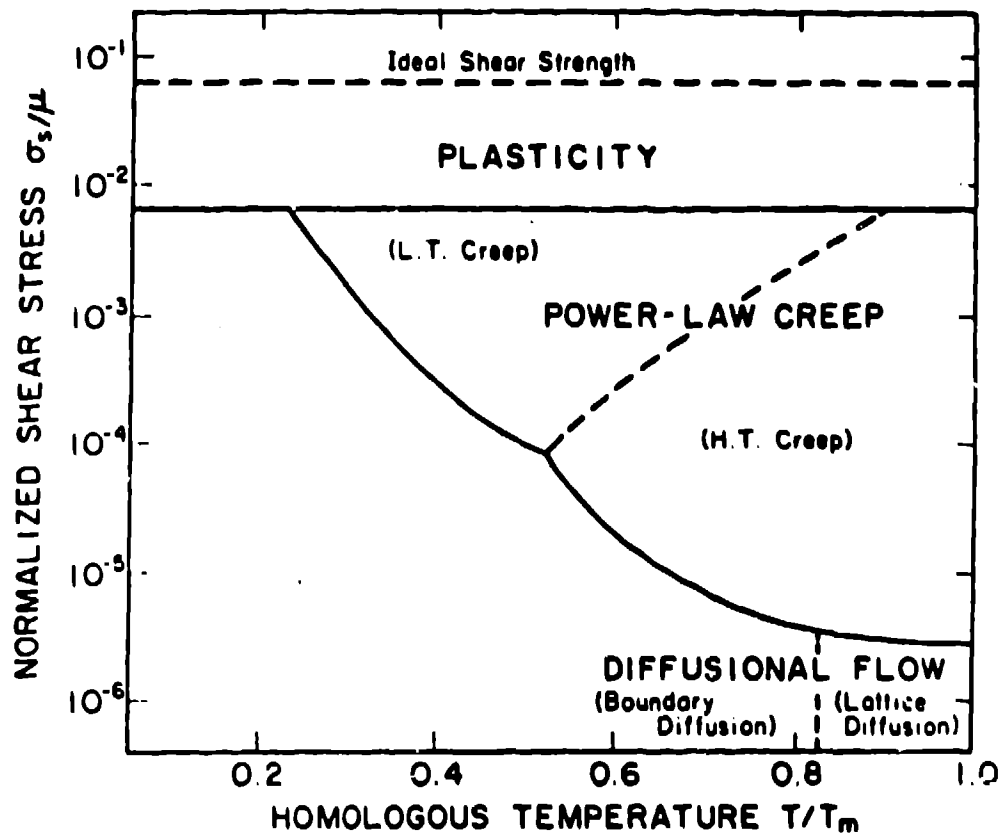


Figure 1 - Schematic Deformation Mechanism Map.

tion glide can be expressed by an expression of the form such as equation 2 (4). Here the most important parameters are the activation energy required to overcome the obstacles to dislocation motion, ΔF , the athermal flow strength, $\bar{\tau}$, which is a measure of the obstacle strength and the applied shear stress, σ_s .

$$\dot{\gamma} = \dot{\gamma}_0 \exp \left[- \frac{\Delta F}{kT} \left(1 - \frac{\sigma_s}{\bar{\tau}} \right) \right] \quad (2)$$

For strong obstacles, ΔF can be as large as $2Gb^3$ or it can be smaller than $0.2Gb^3$ for weak obstacles, where G is the shear modulus. Examples of strong obstacles would include large dispersoids or strong precipitates, whereas weak obstacles would include solute atoms.

At high temperatures ($T > 0.5 T_m$), materials exhibit a strong rate sensitive behavior which is known as creep. This is depicted in Figure 1 as the Power Law Creep regime. The general stress dependence of creep rate is described by an expression of the type shown in equation 3.

$$\dot{\gamma} \propto (\tau_s/G)^\eta \quad (3)$$

The division of the Power Law Creep regime into low temperature and high temperature fields represents the regimes where only dislocation glide occurs and where glide plus dislocation climb occurs, the latter being favored at higher temperatures. As a result of climb in the high temperature Power Law Creep regime, the only effective means of reducing the rate of deformation is to reduce the average lattice diffusivity. This is typically accomplished by adding refractory metal alloying additions to the alloy. Such additions also reduce the creep rate in the regime labeled Diffusional Flow. In this regime the deformation rate is proportional to the effective diffusion coefficient which is a weighted average of the lattice diffusion and the enhanced diffusion at sites such as grain boundaries.

It is significant to note that there is no regime labeled grain boundary sliding. Part of the reason for this is that this mechanism requires both diffusion as well as dislocation motion. Thus, it does not fit into any one regime of Figure 1, and is a function of the processing history, e.g. the grain size.

The Microstructure of Conventional Superalloys

The microstructure of conventional superalloys consists of several main features. These include microstructural constituents such as the coherent phase γ' ($L1_2$ structure, based on $Ni_3(Al,Ti)$) and sometimes γ'' (DO_{22} structure, based on Ni_3Nb) minor intermetallics such as Laves phases and carbides (both at grain boundaries and within the grains). Other features would be grain size and shape. After long term, elevated temperature service, additional phases such as σ and μ can also form and these are known to be detrimental to rupture ductility. Throughout the years, much of the attention on alloy development has been focused on manipulating and controlling these various microstructural features, including suppression of the σ and μ phases. This, coupled with the complimentary attempts to alter and control the other aspects of γ' such as anti-phase boundary energy, represent the majority of the systematic efforts in alloy development for this class of alloys.

As an example, coarsening of the γ' precipitates is a major source of long term microstructural instability during elevated temperature service. It has been shown that the rate of coarsening depends on the state of coherency of the γ' and the lattice and γ phases. Accordingly, considerable

effort has been directed toward gaining an improved understanding of the effects of composition on the misfit of γ' in multi-component alloys. An important aspect of these studies is the determination of solute partitioning between the γ matrix and the γ' precipitates (1,2). For example, in Ni-Al alloys it is known that Cr additions can reduce the γ' misfit as evidenced by a change from cuboidal to spheroidal γ' (Fig. 2(a) and (b)). However, it must be recognized that alloy additions which are added for one purpose can have other effects, some of which may be deleterious. One example is that too much Cr can lead to the formation of the σ -phase (1). As mentioned previously, it is necessary to precipitate a blocky, stable second phase along grain boundaries to minimize sliding and the most common phase which performs this function is a carbide. An example of grain boundary carbides is shown in Figure 2(c). Strong carbide forming elements such as Cr, Nb and Ti are added for this purpose, but it is important to consider the possibility that these elements also might cause deleterious effects. Alloys that contain high concentrations of Nb or Ta can also contain γ'' in addition to γ' as shown in Figures 3(a)-(c).

Finally, there is a group of elements which are added to strengthen grain boundaries but which produce no direct change in the microstructure. These include Mg, Hf and Zr. The need to add these is well documented, yet the absence of an observable microstructural effect suggests that the design of alloys by microstructure control is a necessary but not sufficient approach.

The Constitution in Complex Alloys - Theory vs. Experiment

In addition to the conventional superalloys described above, there is another class of Ni-base alloys that is beginning to receive considerable attention. These alloys contain, among other things, Al and Mo (the latter in high concentration relative to the conventional superalloys). They are interesting in the context of this paper because they are microstructurally complex inasmuch as they typically contain several ordered phases in addition to the γ' . However, the formation and stability of these phases has been the subject of several recent theoretical and experimental studies. These have lead to a semi-quantitative capability for specifying alloy compositions in order to achieve a given constitution. Thus, these alloys represent an example of a class of compositions which can be selected using theoretical concepts for guidance and which have attractive properties (although the properties are not well-understood, at least in terms of microstructure).

The Ni-Al-Mo alloys have been the subject of a large alloy development program because of their excellent high temperature mechanical and physical properties. As a result, there now exists a large body of empirical data regarding composition, constitution and properties. These studies have resulted in selection of several interesting alloy compositions. Two such compositions that have resulted from investigations at Pratt & Whitney Aircraft are shown in Table I. When quenched from 1300°C a large volume fraction of cuboidal γ' precipitates are formed, Figure 4. The fcc γ matrix exhibits a mottled contrast indicative of strain fields caused by incipient precipitation of a second set of ordered phases.

Table I. Typical Compositions of the Ni-Al-Mo-X Superalloys in Atomic Percent

<u>I.D.</u>	<u>Ni</u>	<u>Al</u>	<u>Mo</u>	<u>Ta</u>	<u>W</u>	<u>C</u>
RSP 143	76	13	9	2	-	-
RSR 185	73.8	15	9	-	2	0.2

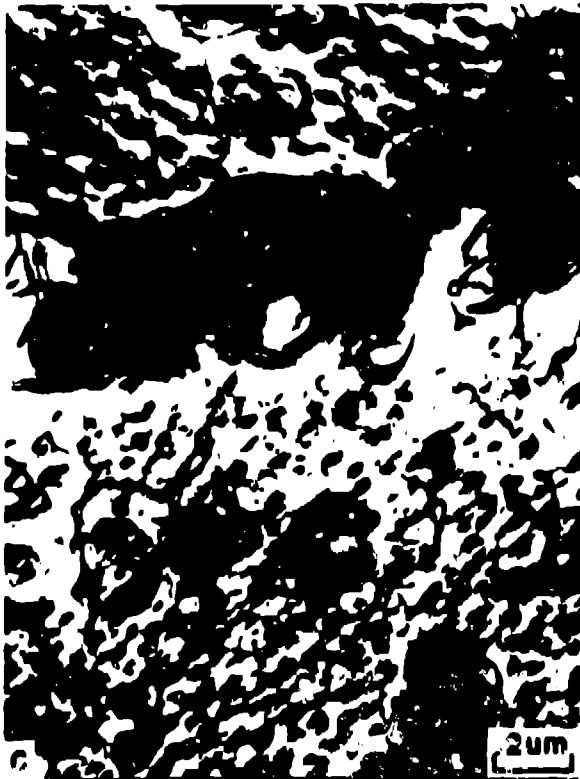
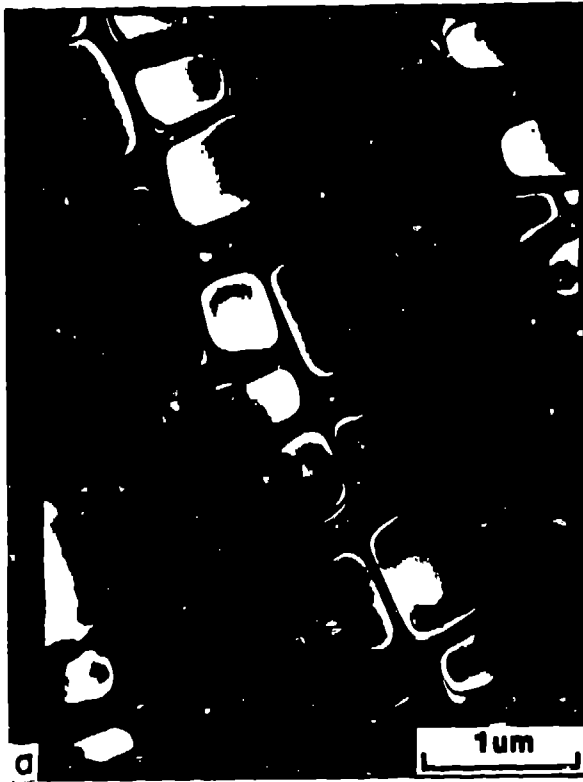


Figure 2 - Typical microstructural features in conventional superalloys.
a) cuboidal γ' in cast Mar-M-247 (dark field using (100) γ' reflection).
b) spheroidal γ' in wrought Waspalloy (dark field using (100) γ' reflection).
c) grain boundary carbides in wrought Waspalloy (bright field micrograph).

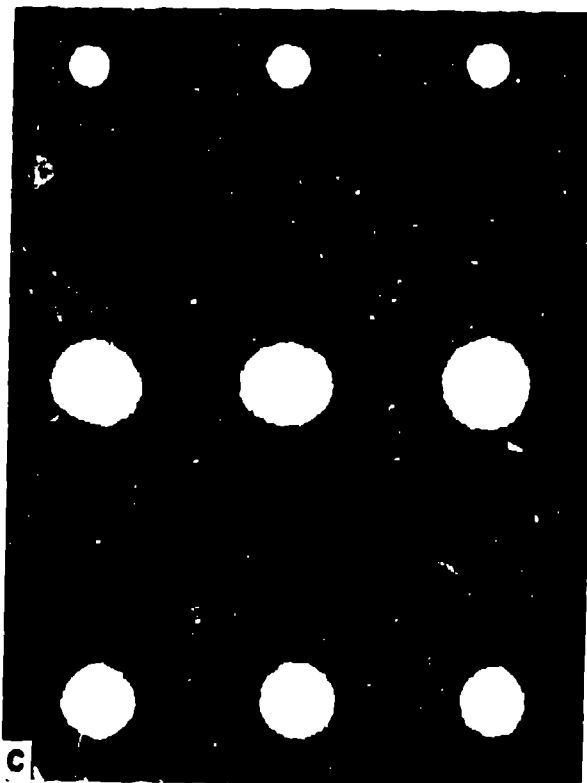


Figure 3 - Dark field micrographs showing coexistence of γ' and γ'' in wrought Inco 718.

- a) γ'' DF using $\frac{1}{4}$ (420) matrix position
- b) γ' using $\frac{1}{2}$ (220) matrix position
- c) selected area electron diffraction pattern, [211] matrix zone normal.

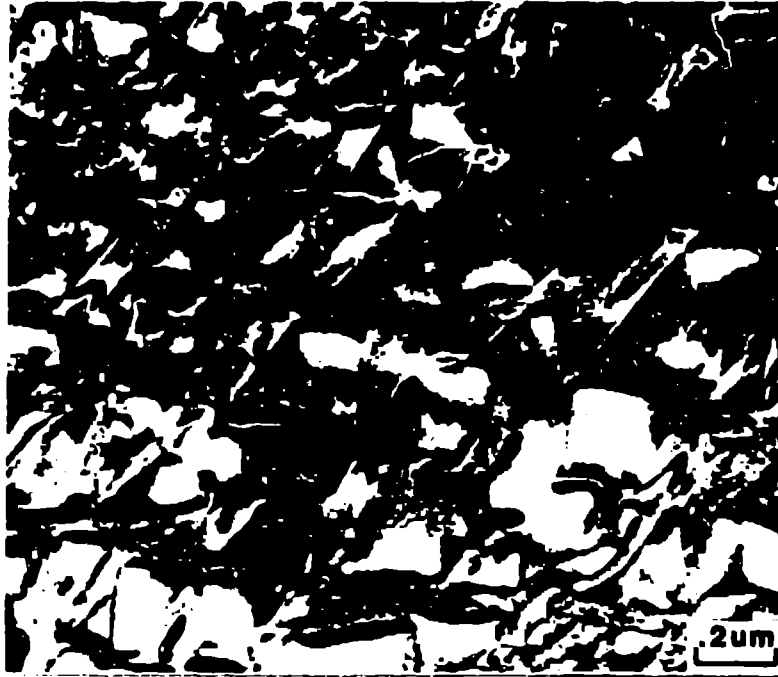


Figure 4 - Bright field TEM image of the γ' precipitates in RSR 185 as-quenched from 1300°C, ($g = (200)$ off $[001]$ zone).

Aging these quenched alloys at an elevated temperature causes long range ordered phases to form in the γ matrix which remains between the γ' precipitates. Depending on the alloy composition, these precipitates can form with several different structures each based on the Ni_xMo ($x = 2,3$ or 4) stoichiometry (7,8). Comparing the indexed electron diffraction patterns shown in Figure 5 to those obtained from alloys 143 and 185 quenched and aged at $700^\circ C$ illustrates this point, Figures 6 and 7. The W bearing quaternary (alloy 185) forms the DO_{22} (A_3B stoichiometry) and the Pt_2Mo (A_2B stoichiometry) structures, while the Ta bearing quaternary (alloy 143) initially forms the DO_{22} and on further aging forms the $D1a$ (A_4B stoichiometry) structures. In each case, these precipitates coexist with the γ' particles as shown by the dark field images of the Ni_xMo precipitates in Figure 8.

It is extremely difficult to understand complex compositional effects on structure in quaternary alloys. However, the problem can be simplified by noting that, following the formation of the γ' , the remaining γ matrix has the appropriate composition $Ni_3(Mo,X)$ where X corresponds to either Ta or W (9). Thus, the effect of composition on structure can be studied by modeling the phase transitions taking place in the γ matrix of the quaternary superalloys with monolithic ternary alloys based on $Ni_3(Mo,X)$. Additionally, we will show in the following paragraphs that the transformations observed in these ternaries can be rationalized by their similarity to the ordering reaction in a binary Ni-25at%Mo alloy. In this way, a connection can be made between theory calculations and transformation studies performed on binary alloys and the structures observed in technologically important quaternary alloys which contain γ' and Ni_xMo .

The compositions of three of the $Ni_3(Mo,X)$ alloys studied are shown in Table II. Roughly 3 atomic percent Al and Ta and 5 atomic percent W were substituted for Mo while maintaining the $Ni_3(Mo,X)$ stoichiometric ratio. Thin samples of these alloys were quenched from the fcc phase field ($1300^\circ C$) into iced brine (9). Selected area electron diffraction showed the existence of diffuse intensity at the $\{1 \frac{1}{2} 0\}$ locations of reciprocal space, Figure 9. This diffuse intensity has been attributed to short range order associated with the $\{1 \frac{1}{2} 0\}$ special point (10-13) and has been extensively studied by electron diffraction (14-16).

Table II. $Ni_3(Mo,X)$ Powder Compositions in Atomic Percent

<u>Ni</u>	<u>Mo</u>	<u>C</u>	<u>N</u>	<u>O</u>	<u>P</u>	<u>S</u>	<u>X</u>
75.3	21.8	.033	.024	.071	.009	.004	2.72 Al
74.9	21.9	.047	.025	.097	.009	.004	2.97 Ta
74.8	20.1	.012	.026	.064	.009	.004	5.05 W

When these quenched alloys are subsequently heated to moderate temperatures, the short range ordered matrix decomposes into one or more of the Ni_xMo long range ordered structures previously described (17). Figure 10 shows the structures which have formed after 10 hours at $700^\circ C$ in the three ternary alloys. Careful comparison of Figure 10 with Figure 5 shows the following: (1) the Pt_2Mo structure is present in all of the alloys; (2) the DO_{22} structure is stable in the Al bearing alloy; (3) the $D1a$ structure is present in the W bearing ternary; and (4) the ternary alloy containing Ta shows evidence of both the DO_{22} and $D1a$ structures. The evolution of the long range ordered structures in the W bearing ternary is indistinguishable from binary Ni_3Mo , i.e. the Pt_2Mo and $D1a$ (Ni_2Mo and Ni_4Mo stoichiometries) form in equal proportions as metastable phases prior to the nucleation of

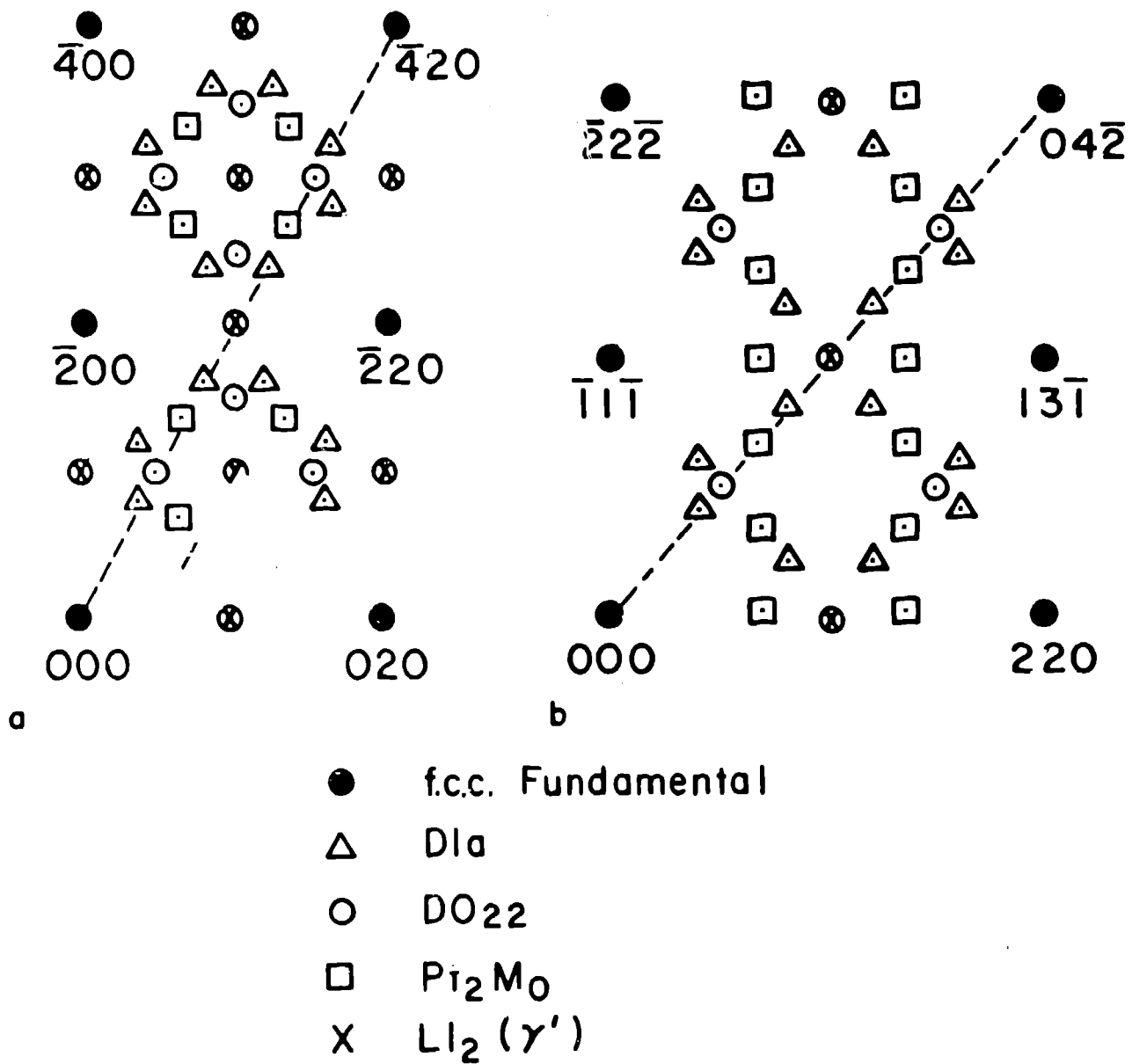


Figure 5 - Composite selected area electron diffraction patterns to, the case when all Ni_xMo phases are present along with the γ' phase, a) [001] b) [112] zone

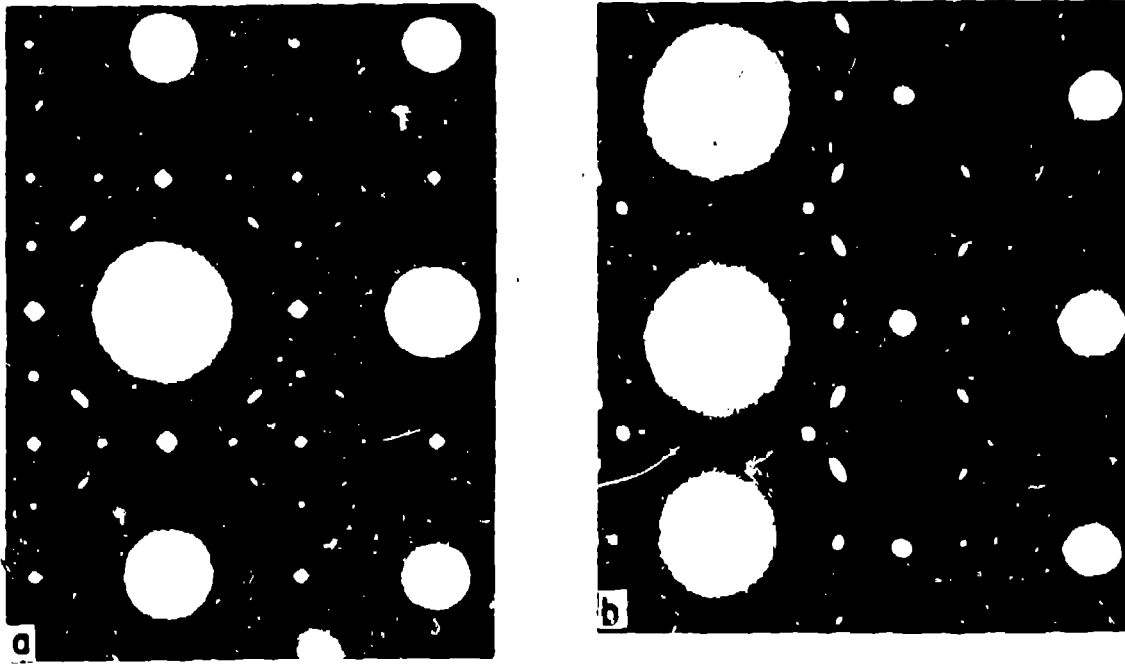


Figure 6 - Diffraction patterns from PSR 185 quenched and aged at 700°C,
 a) 10 hours [001] zone b) 100 hours [112] zone.

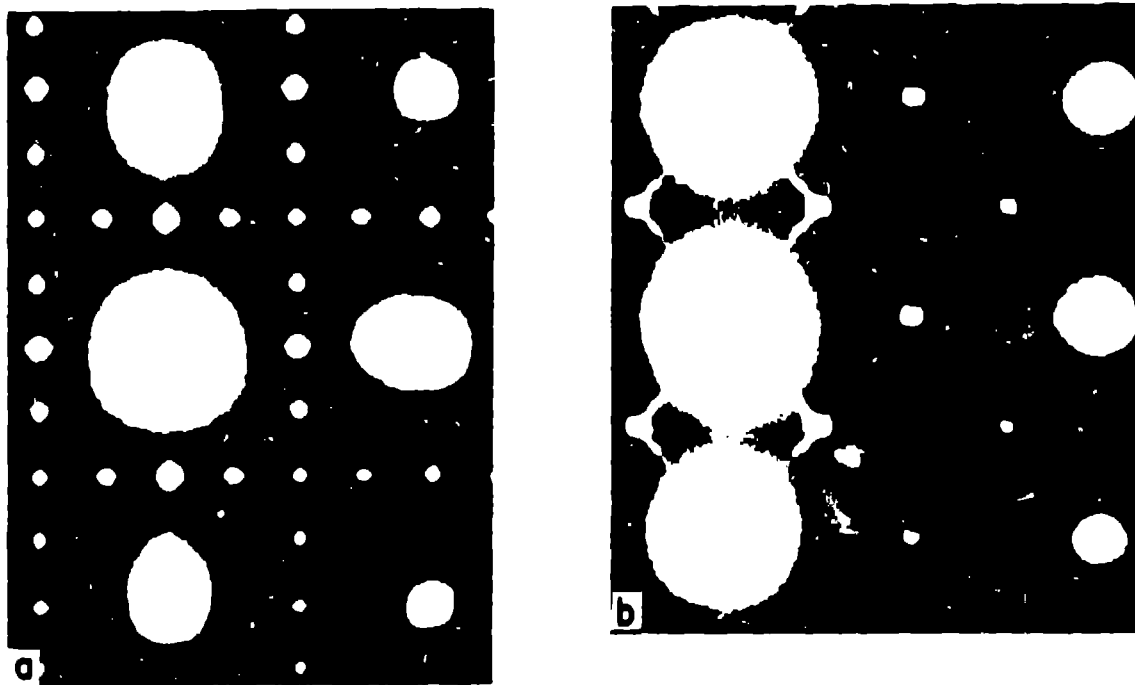


Figure 7 - Diffraction patterns from RSR 143 quenched and aged at 700°C,
 a) 10 hours [001] zone (b) 100 hours [112] zone.

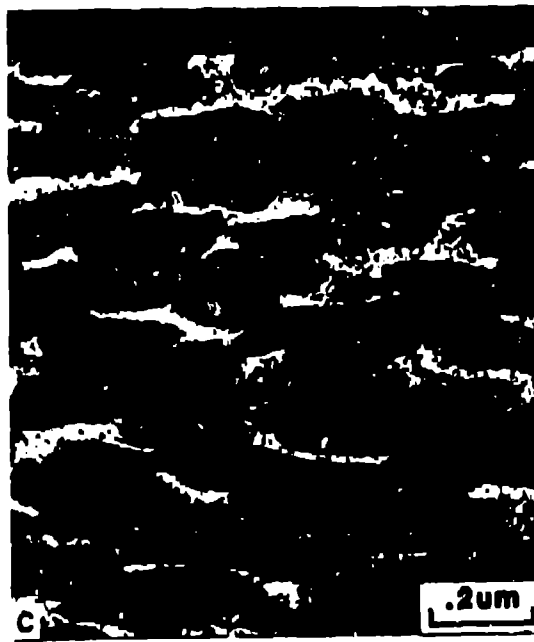
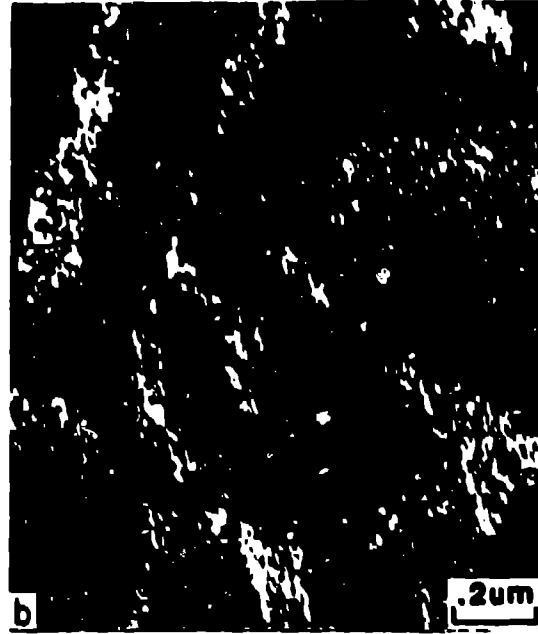


Figure 8 - Dark field TEM images of the Ni_xMo precipitates following aging at $700^{\circ}C$ for 100 hours, a) DO_{22} in RSR 185 b) Pt_2Mo in RSR 185 c) DO_{22} in RSR 143.

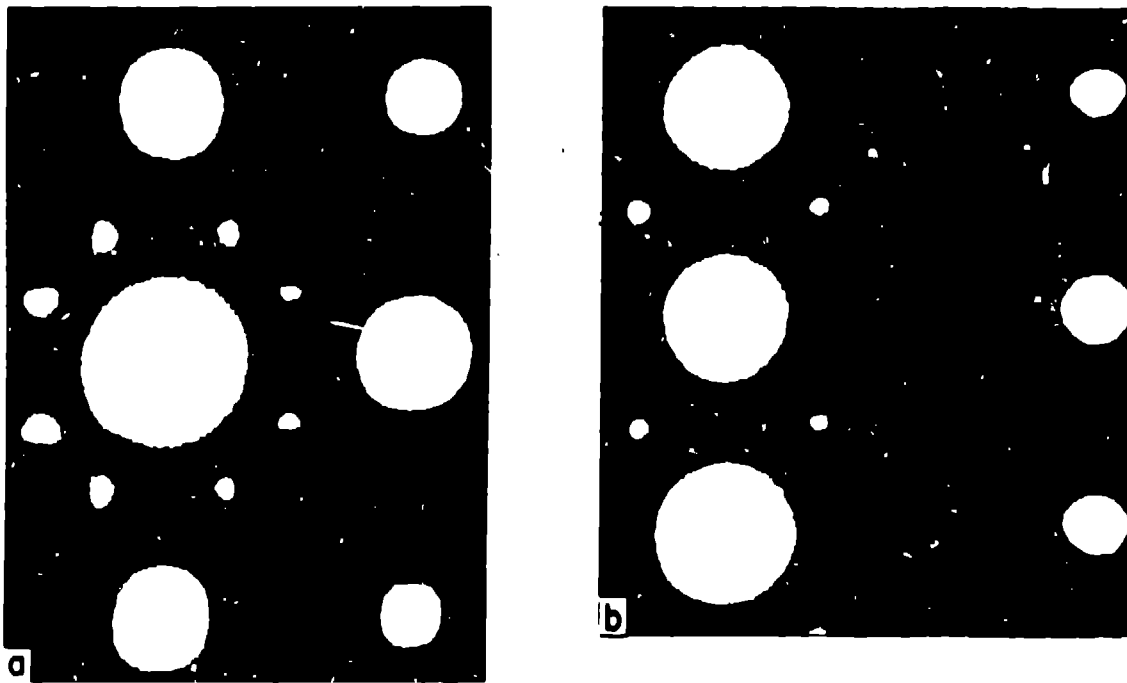


Figure 9 - Diffraction patterns showing the $\{1 \frac{1}{2} 0\}$ diffuse intensity following quenching from 1300°C, a) $\text{Ni}_3(\text{Mo},\text{W})$ [001] zone b) $\text{Ni}_3(\text{Mo},\text{Ta})$ [112] zone.

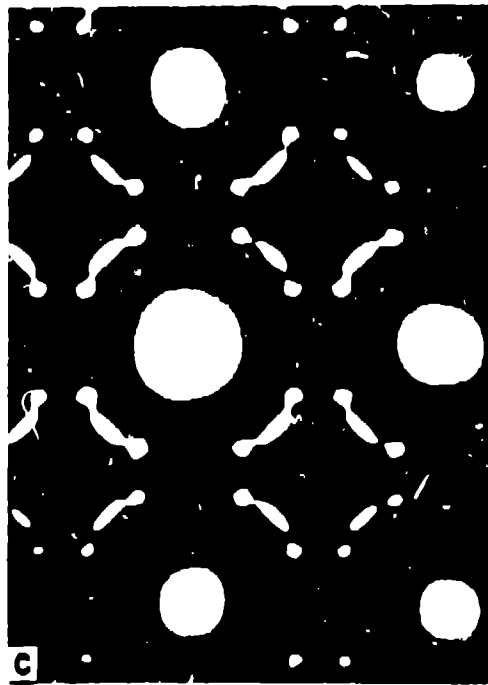
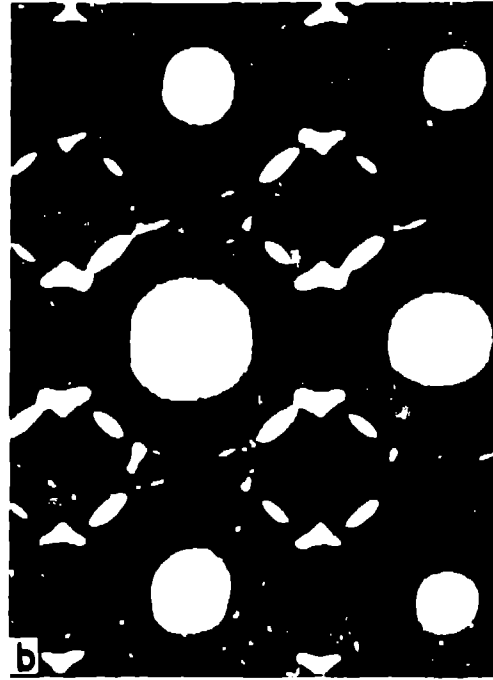
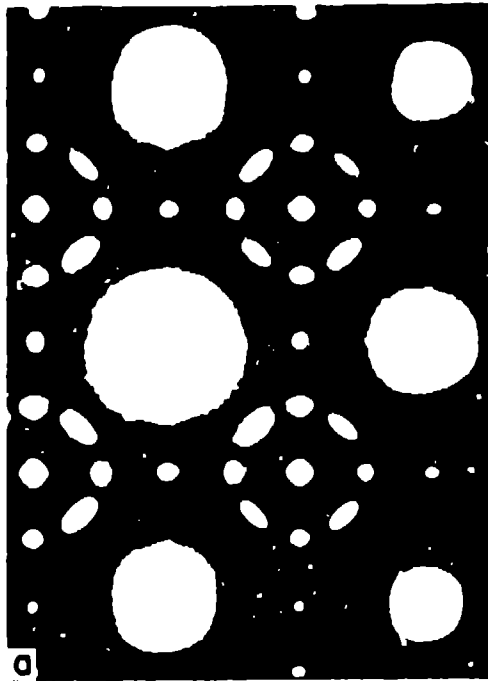


Figure 10 - [001] zone diffraction patterns from the $\text{Ni}_3(\text{Mo},\text{X})$ alloys quenched and aged at 700°C for 10 hours, a) $\text{Ni}_3(\text{Mo},\text{Al})$ b) $\text{Ni}_3(\text{Mo},\text{Ta})$ c) $\text{Ni}_3(\text{Mo},\text{W})$.

the equilibrium orthorhombic Ni_3Mo (18). In contrast to this, the Al and Ta additions stabilize, to various degrees, the DO_{22} (Ni_3Mo stoichiometry) structure. The DO_{22} structure has been observed in binary Ni_3Mo as a metastable species only when thin foils have been treated in-situ in the electron microscope (19). Thus, Al, and to a lesser extent Ta, change the energetics of the system to favor the formation of the DO_{22} structure relative to, or in competition with, the Pt_2Mo and D1a structures.

In order to explain the effects of relatively small ternary additions, one must rely on the extensive alloy theory literature pertinent to the Ni-Mo, or more generally the $\{1 \frac{1}{2} 0\}$, class of alloys. Using pairwise approximations to interatomic bonding in alloys, the four regions of fcc ordering have been determined using ratios of the first (V_1), second (V_2) and third (V_3) neighbor interactions (11). When interactions beyond the second nearest neighbor are ignored, the long range ordered structures having the minimum configurational energy at 0°K have been determined by Cahn and co-workers (20-22). Figure 11 is taken from this work and shows the ground states for the portion of V_2/V_1 space pertinent to the $\{1 \frac{1}{2} 0\}$ alloys as a function of composition. The contribution of configurational entropy to the free energy of these ground states has been calculated by Sanchez and deFontaine (23). They used the data to plot the idealized temperature/composition (coherent) phase diagrams shown in Figure 12 (23,24).

A significant limitation of the theory described above is that it excludes the D1a (Ni_4Mo) phase from consideration. This is because it has been shown that fourth nearest neighbor interactions must be considered for the D1a structure to be considered as a unique ground state structure (25). When only V_1 and V_2 are considered, the region between 0.16 and 0.25 atomic percent B (cross hatched area of Figure 11) is degenerate with respect to mixtures of A_5B , A_4B and A_3B . Thus, Sanchez and deFontaine could not include the D1a structure in their phase diagram calculations for reasons of numerical convergence. Since this structure figures prominently in the experimental observations of Ni-Mo ordering, (and the A_5B structure has never been observed), the absence of the D1a structure from the theoretical calculations is unfortunate. Nevertheless, this rather involved background makes it possible to begin to explain some of the observations obtained from the $\text{Ni}_3(\text{Mo},\text{X})$ alloys. If these can be approximated as pseudo-binaries, then it is possible to explain some of the effects of the ternary additions by changes in V_2/V_1 (9,17). In a very qualitative sense, Sanchez and deFontaine showed that lowering V_2/V_1 increases the stability of the $\text{DO}_{22}(\text{A}_3\text{B})$ structure relative to the $\text{Pt}_2\text{Mo}(\text{A}_2\text{B})$ structure, Figure 12. Figure 10 shows that the substitution of Al for Mo has this same effect when compared to the W substitution. Thus, it can be inferred that Al lowers the V_2/V_1 ratio from its value in the $\text{Ni}_3(\text{Mo},\text{W})$ ternary or binary Ni_3Mo (15,17).

The analysis which produced the coherent phase diagrams allows some conclusions to be made concerning the mechanism of the transition. The dashed lines in Figure 12 are the locus of the $\{1 \frac{1}{2} 0\}$ spinodal ordering instability (10). By noting the intensification of the $\{1 \frac{1}{2} 0\}$ diffuse intensity during the early stages of decomposition, it is possible to determine whether the aging temperature is above or below this locus (9). Using this technique, it has been shown that 800°C is above this instability for $\text{Ni}_3(\text{Mo},\text{Al})$ and below it for $\text{Ni}_3(\text{Mo},\text{Ta})$ and $\text{Ni}_3(\text{Mo},\text{W})$ (17). If the ternary elements change the ratio of V_2 to V_1 , then the $\{1 \frac{1}{2} 0\}$ spinodal instability should be a function of this ratio as is predicted in Figure 12.

Using the results from the $\text{Ni}_3(\text{Mo},\text{X})$ alloys, it is possible to explain the general trends seen in the Ni-Al-Mo-X superalloys. Since Al and Ta both favor the stability of the DO_{22} structure relative to the Pt_2Mo (Fig. 10), it is not surprising that alloy 143 (Ni-Al-Mo-Ta) forms the DO_{22} structure and not the Pt_2Mo (Fig. 7). Conversely, since W in Ni_3Mo does not change its propensity to form the D1a and Pt_2Mo structures, alloy 185 (Ni-Al-Mo-W) forms

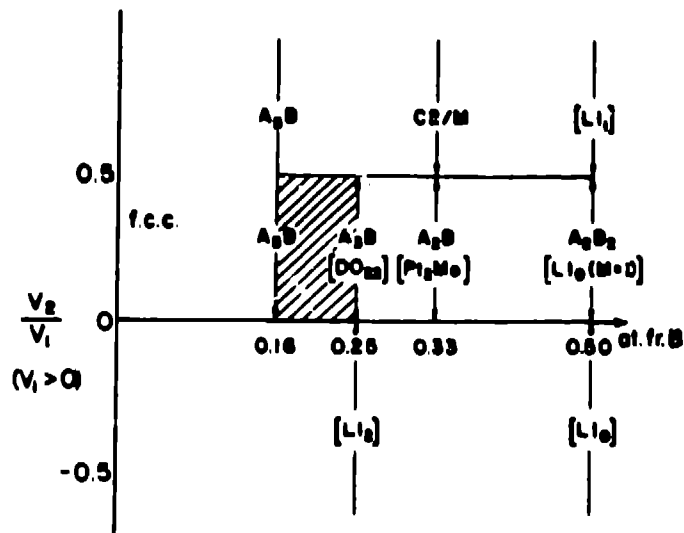


Figure 11 - Structures with the minimum configurational free energy at 0°K versus the ratio of the second to first nearest neighbor interaction parameter (after Cahn and coworkers (refs. 20,21,22)).

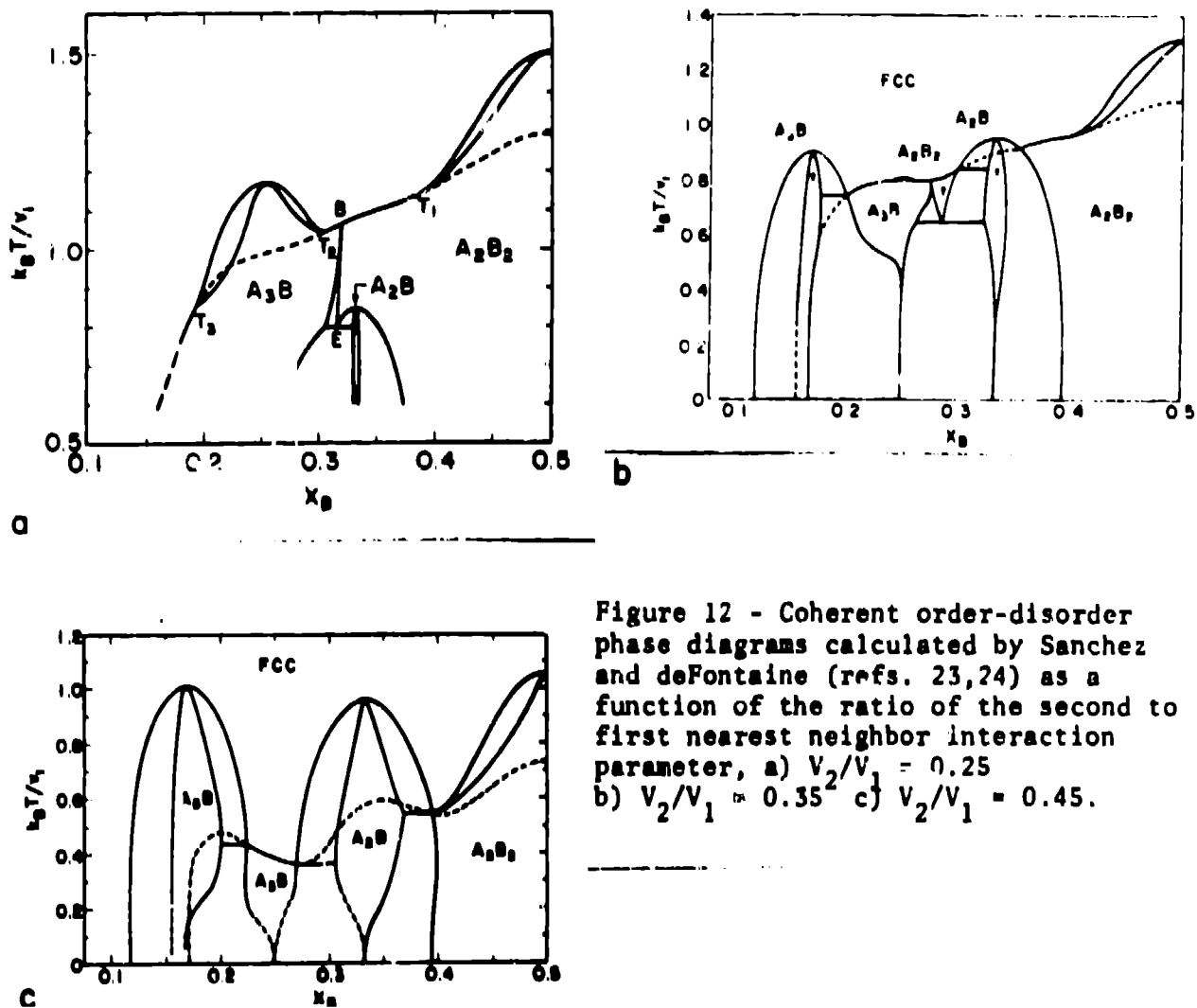


Figure 12 - Coherent order-disorder phase diagrams calculated by Sanchez and deFontaine (refs. 23,24) as a function of the ratio of the second to first nearest neighbor interaction parameter, a) $V_2/V_1 = 0.25$ b) $V_2/V_1 = 0.35$ c) $V_2/V_1 = 0.45$.

both the DO_{22} and the Pt_2Mo structures. The DO_{22} stability may arise from the finite Al content in the γ matrix following the γ' formation.

There seems to be a delicate balance between the compositional factors which favor the various Ni_xMo phases. As a result, different of these phases can be formed by relatively minor composition changes in this class of superalloys. For the "alloy designer" to approach the task of selecting optimal combinations he needs several diverse pieces of information. A partial list might include the following:

- 1) the mechanical properties of each alloy constituent,
- 2) the thermal stability of each phase,
- 3) the compositional boundaries for stability of each precipitate, and
- 4) the morphology and coherency (as influenced by the mechanism of the transformation) for each constituent,
- 5) partitioning of solute between the γ' and the matrix.

To approach these complex questions, the choice is between empiricism or attempting to simplify the system in order to apply alloy theory as it is known today. All too often, time constraints dictate that the former approach is taken rather than the latter. Hopefully, as the theories approach viability in more useful alloy systems, more sophisticated techniques will be used to simplify complex microstructures in order to study their constituent parts. Then and only then can theory and experiment approach the common ground where meaningful interactions can occur.

References

1. "Alloy and Microstructural Design," J. K. Tien and G. S. Ansell, eds., Academic Press, New York, NY, 1976.
2. "The Superalloys," C. T. Sims and W. C. Hagel, eds., John Wiley & Sons, New York, NY, 1972.
3. "Metallurgical Treatises," J. K. Tien and J. F. Elliott, eds., TMS-AIME, Warrendale, PA, 1981.
4. "Deformation-Mechanism Maps," H. J. Frost and M. F. Ashby, eds., Pergamon Press, New York, NY, 1982.
5. J. Weertman, Trans. Met. Soc. AIME, 227, 1475 (1963).
6. M. F. Ashby, Acta Met., 20, 887 (1972).
7. P. L. Martin and J. C. Williams, in Solid-Solid Phase Transformations, H. I. Aaronson, D. E. Laughlin, R. F. Sekerka and C. M. Wayman, eds., TMS-AIME, Warrendale, PA, 1982, p 757.
8. E. H. Aigeltinger, S. R. Bates, R. W. Gould, J. J. Hren and F. N. Rhines, in Rapid Solidification Processing Principles and Technologies, Claitor's, New York, NY, 1978, p 291.
9. P. L. Martin, Ph.D. Dissertation, Carnegie-Mellon University, Pittsburgh, PA, 1982.
10. D. deFontaine, Acta Met., 23, 553 (1975).
11. P. C. Clapp and S. C. Moss, Phys. Rev., 142 (1966), p 418.
12. P. C. Clapp and S. C. Moss, Phys. Rev., 171 (1968), p 754.
13. S. C. Moss and P. C. Clapp, Phys. Rev., 171 (1968), p 764.
14. R. deKiddler, G. vanTendeloo and S. Amelinckx, Acta. Cryst., A32 (1976), p 216.
15. S. K. Das, P. R. Okamoto, P.M.J. Fisher and G. Thomas, Acta Met., 21 (1973), p 913.
16. W. M. Stobbs and J.-P. Chevalier, Acta Met., 26 (1978), p. 233.
17. P. L. Martin and J. C. Williams, Acta Met., in press.
18. M. Yamamoto, N. Soji, T. Saburi and Y. Mizutani, Trans. JIM, 11, (1970), p 120.

19. G. van'tendeloo, R. deRidder and S. Amelinckx, Phys. Stat. Sol. (a), 27 (1975) p 457.
20. M. J. Richards and J. W. Cahn, Acta Met., 19 (1971), p 1263.
21. S. M. Allen and J. W. Cahn, Acta Met., 20 (1972), p 423.
22. S. M. Allen and J. W. Cahn, Scripta Met., 7 (1973), p 1261.
23. J. M. Sanchez and D. deFontaine, Phys. Rev. B, 25 (1982), p 1759.
24. D. deFontaine, Met. Trans., 12A, (1981), p 559.
25. J. Kanamori and Y. Kakehashi, Journal de Physique (Paris), 38, Coll. C-7, (1977), p 274.